HHS Public Access

Author manuscript

J Am Chem Soc. Author manuscript; available in PMC 2024 August 20.

Published in final edited form as:

J Am Chem Soc. 2024 July 31; 146(30): 21061–21068. doi:10.1021/jacs.4c06411.

Biosynthesis of the Unusual Epoxy Isonitrile-Containing Antibiotics Aerocyanidin and Amycomicin

Ziyang Zheng,
Department of Chemistry, University of Texas at Austin, Austin, Texas 78712, United States

Jon Clardy,
Department of Biological Chemistry and Molecular Pharmacology, Harvard Medical School and Blavatnik Institute, Boston, Massachusetts 02115, United States

Hung-wen Liu
Department of Chemistry, University of Texas at Austin, Austin, Texas 78712, United States; Division of Chemical Biology and Medicinal Chemistry, College of Pharmacy, University of Texas at Austin, Austin, Texas 78712, United States

Abstract

Aerocyanidin and amycomicin are two antibiotics derived from long-chain acids with a rare epoxy isonitrile moiety, the complexity of which renders the total synthesis of these two natural products rather challenging. How this functionality is biosynthesized has also remained obscure. While the biosynthetic gene clusters for these compounds have been identified, both appear to be deficient in genes encoding enzymes seemingly necessary for the oxidative modifications observed in these antibiotics. Herein, the biosynthetic pathways of aerocyanidin and amycomicin are fully elucidated. They share a conserved pathway to isonitrile intermediates that involves a bifunctional thioesterase and a nonheme iron α-ketoglutarate-dependent enzyme. In both cases, the isonitrile intermediates are then loaded onto an acyl carrier protein (ACP) catalyzed by a ligase. The isonitrile-tethered ACP is subsequently processed by polyketide synthase(s) to undergo chain extension, thereby assembling a long-chain γ-hydroxy isonitrile acid skeleton. The epoxide is installed by the cupin domain-containing protein AecF to conclude the biosynthesis of aerocyanidin. In contrast, three P450 enzymes AmcB, AmcC, and AmcQ are involved in epoxidation and keto formation to finalize the biosynthesis of amycomicin. These results thus explain the sequence of oxidation events that result in the final structures of aerocyanidin and amycomicin as well as the biosynthesis of the key γ-hydroxy epoxy isonitrile functional group.

Corresponding Author: Hung-wen Liu − Department of Chemistry, University of Texas at Austin, Austin, Texas 78712, United States; Division of Chemical Biology and Medicinal Chemistry, College of Pharmacy, University of Texas at Austin, Austin, Texas 78712, United States; h.w.liu@mail.utexas.edu.

Supporting Information

The Supporting Information is available free of charge at https://pubs.acs.org/doi/10.1021/jacs.4c06411.
Additional experimental details, materials, and methods, including chemical synthesis, gene deletion and complementation, heterologous expression experiments, protein purification, in vitro enzymatic assays, supplementary tables and figures, and NMR spectra for synthetic compounds (PDF)

Complete contact information is available at: https://pubs.acs.org/10.1021/jacs.4c06411

The authors declare no competing financial interest.

Graphical Abstract

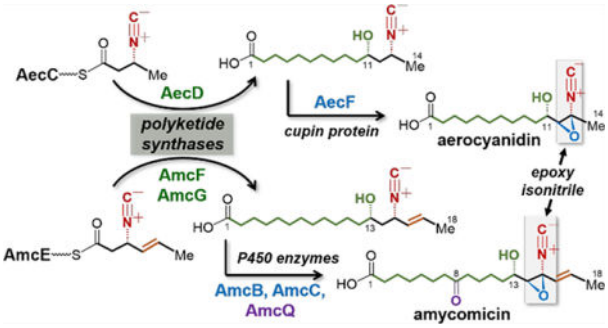

INTRODUCTION

Aerocyanidin (**1**),[1] YM-47515 (**2**)[2] and amycomicin (**3**)[3] isolated from *Chromobacterium violaceum*, *Micromonospora echinospora* and *Amycolatopsis* sp. AA4, respectively, are the only three long-chain fatty acid derivatives featuring a γ-hydroxyl-α,β-epoxy isonitrile functionality (Figure 1A). These natural products are antibiotics showing activity against Grampositive bacteria including several methicillin-resistant *Staphylococcus aureus* (MRSA) strains.[1–3] Both YM-47515 (**2**) and amycomicin (**3**) are homologues of aerocyanidin (**1**) with their chains extended by two and four more carbons, respectively. Amycomicin also contains an extra carbonyl group at C8 and an olefin moiety between C16 and C17 compared to aerocyanidin and YM-47515. The epoxy isonitrile group is known to be essential for the antimicrobial activity of these compounds,[4] and amycomicin has recently been shown to target FabH in fatty acid biosynthesis such that it holds promise to treat infections with *S. aureus*.[3] Chemical preparation of this class of compounds has been challenging due to instability of the γ-hydroxyl-α,β-epoxy isonitrile moiety, which can readily undergo Payne rearrangement (**5** → **6**) under both alkaline and acidic conditions, resulting in an epoxy ketone product with concomitant release of cyanide (Figure 1C).[4] Nevertheless, trichoviridin (**4**),[5,6] a highly functionalized epoxy isonitrile-containing cyclopentane natural product useful for the control of crop pathogens,[7] has been successfully synthesized by Baldwin and co-workers.[8] Despite this progress, how the rare and highly reactive epoxy isonitrile moiety in these secondary metabolites is biosynthesized remains largely unexplored.

The gene clusters, *aec* and *amc*, for the production of aerocyanidin (**1**) and amycomicin (**3**), respectively, have recently been identified by Clardy and co-workers (Figure 2A).[3] The presence of polyketide synthase (PKS) genes (*aecD* and *amcF/G*) in these clusters suggests that the backbone in **1** and **3** does not originate entirely from fatty acid biosynthesis as previously surmised but also polyketide biosynthesis. Both clusters are in part homologous to the *sco* and *mma* gene clusters from *Streptomyces coeruleorubidus* and *Mycobacterium marinum*, respectively. Among them, the *sco* cluster is involved in the biosynthesis of the isonitrile lipopeptide (INLP) 7, while the *mma* cluster is proposed to produce **8** (Figures 1B and 2A).[9] Importantly, the functions of the gene products encoded in the *sco* and *mma* clusters have been fully established by Zhang and co-workers.[9,10] As illustrated in Figure 2B, biosynthesis of INLP-1 (**7**) begins with the ScoC-mediated loading of crotonic

acid (**9**) onto the acyl carrier protein (ACP) ScoB. The bifunctional thioesterase ScoD then catalyzes a Michael addition of glycine (**11**) to the crotonyl-ScoB (**10**) followed by hydrolysis of the thioester bond of **12** to give **13**. Subsequent oxidation catalyzed by the nonheme iron α-ketoglutarate-dependent (Fe/α-KG) enzyme ScoE converts **13** to the isonitrile product **14**. Compound **14** will be reloaded onto ScoB and processed by the nonribosomal peptide synthetase (NRPS) ScoA to yield the final product 7 (Figure S2). The four genes *scoB*/*C*/*D*/*E* in the *sco* cluster are conserved in the *aec* and *amc* gene clusters, corresponding to *aecC*/*E*/*B*/*A* and *amcE*/*H*/*D*/*A*, respectively. This gene conservation implies that biosynthesis of the isonitrile moieties in **1** and **3** may involve a similar series of reactions (Figure 2B).

While previous study of INLP biosynthesis has shed light on isonitrile formation in aerocyanidin and amycomicin, how the hydroxyl group as well as the epoxide are introduced in **1** and **3** remains obscure. In particular, aerocyanidin biosynthesis involves three oxidation reactions including isonitrile formation, C12−C13 epoxidation and C11 hydroxylation; yet, there are only two putative oxidase genes (i.e., *aecA* and *aecF*) in the cluster and the *aecA*-encoded gene product has already been assigned to isonitrile formation.[11] Interestingly, compared with the *aec* cluster, the *amc* cluster has an *aecA* homologue (*amcA*), but no *aecF* gene homologue, which suggests a distinct difference between amycomicin biosynthesis and that of aerocyanidin, especially since the former is more oxidized than the latter. In addition to isonitrile formation which likely involves *amcA*, six two-electron oxidations of the backbone are expected to install the C8 ketone, C13 hydroxyl, C14−C15 epoxide, and C16−C17 double bond in **3** (see arrows in Figure 1A). However, only three oxidase genes (i.e., *amcB*, *amcC* and *amcQ*), which all encode P450 enzymes, can be located in the *amc* cluster. Moreover, it is not apparent why the *amc* cluster also includes six genes normally associated with fatty acid biosynthesis (FAB) (i.e., *amcK*, *amcL*, *amcM*, *amcN*, *amcO* and *amcS*) as the long-chain acid backbone of amycomicin (**3**) is likely derived from a polyketide. The present work addresses these questions investigating the activity of the putative oxidases in vitro along with several other enzymes encoded in the gene clusters and thereby establishing the aerocyanidin and amycomicin biosynthetic pathways.

RESULTS AND DISCUSSION

To study the proposed functions of AecA/B/C/E, these four proteins were heterologously overexpressed and purified from *Escherichia coli* as *N*-His_6-tagged constructs and assayed in vitro. Co-incubation of the putative ligase AecE with crotonic acid (**9**), the ACP AecC (*apo* form), coenzyme A (CoA), phosphopantetheinyl transferase (Sfp), ATP, and $MgCl_2$ did not yield the anticipated crotonyl-AecC adduct. Inclusion of the reductant tris(2-carboxyethyl)phosphine (TCEP) in the preceding assay did not produce crotonyl-AecC, either. It is thus possible that formation of crotonyl-AecC may not be required in the pathway. Considering that crotonyl-CoA (**15**) is a common intermediate in fatty acid metabolism,[12] crotonyl-CoA instead of crotonyl-AecC may instead be the substrate of AecB. To test this hypothesis, *N*-acetylcysteamine activated crotonic acid (**16**, the SNAc analog of crotonyl-CoA) was synthesized and incubated with AecB as well as glycine (**11**). In this case, the glycine adduct **13** was indeed produced as shown in Figure S3A. The fact

that **16** can be processed by AecB indicated that crotonyl-CoA is likely the true substrate for AecB in vivo. Marfey's analysis[13] revealed that the stereochemistry at C3 in **13** is *R* (Figure S4A). Moreover, coincubation of chemically synthesized **13** with AecA, α-KG, $Fe(NH_4)_2(SO_4)_2$, and ascorbic acid resulted in isonitrile formation to yield **14** (Figure S3B). The stereochemistry of C3 was the same in both **13** and **14** (Figure S4B). These results are consistent with a pathway in which the isonitrile **14** serves as a common intermediate in the biosynthesis of both INLP-1 (**7**) and aerocyanidin (**1**). However, formation of crotonyl-AecC appears to be unnecessary in the latter pathway.

During the biosynthesis of **7**, ScoC catalyzes reloading of **14** onto the ACP ScoB. The resulting **14**-ScoB is then processed by the NRPS ScoA followed by reductive release from ScoA catalyzed by its own reductase domain to generate the final product **7** (Figures 2B and S2).[9,10] It was thus hypothesized that the ligase AecE may catalyze ligation of **14** with the ACP AecC in the aerocyanidin pathway. Indeed, **14**-tethered AecC (**17**) was observed when **14** was incubated with AecC and AecE (Figure 3A,C). The presence of the type I PKS gene *aecD* in the cluster suggested that **17** may be the starter unit for polyketide chain extension catalyzed by AecD to generate the hydrocarbon chain in **1.** Based on this assumption, the C11 hydroxyl group in aerocyanidin may thus result from β-keto reduction catalyzed by the ketoreductase (KR) domain of AecD in the first round of chain elongation (**18** → **19**, Figure 3C). The following four rounds of extension would furnish the 14-carbon skeleton of **1** (**19** → **24**, Figure 3C). In order to test this hypothesis, *aecD* was heterologously coexpressed with *aecABCE* in *E. coli* K207. LCMS analysis of the culture medium identified a species with the same molecular weight as **24** (calcd for $C_{15}H_{26}NO_3^-$ $[M-H]^-$: 268.1918, found: 268.1916, Figure 3B). Furthermore, it also has an identical retention time with the chemically synthesized standard of **24**. In the absence of *aecD*, this species was absent, indicating that production of this species is *aecD*-dependent (Figure 3B).

In order to better characterize the chain elongation process, AecD was isolated from *E. coli* as a recombinant *N*-His_6-tagged construct and incubated with chemically prepared **14**, CoA, *apo*-AecC, $MgCl_2$, TCEP, Sfp, ATP, AecE, malonic acid, the malonyl CoA synthetase MatB, and NADPH. The reaction mixture was analyzed by LCMS after hydrolysis of the thioester bonds to release the products from AecD at pH 9.5. As shown in Figure 4A, **24** was observed consistent with the preceding heterologous expression experiments. Moreover, the C11 stereochemistry of **24** is *S* as its C11-epimer (11-*epi*-**24**) has a different retention time (Figure S5). The *S*-configuration at C11 of **24** is also consistent with the prediction based on sequence analysis of the reductase domain of AecD, which harbors the conserved Asp residue that dictates the stereoselectivity to generate D-hydroxyl groups (Figure S6).[14,15] Besides, intermediates with various carbon chain lengths were also identified by comparison with the reaction using [2-^{13}C]-malonic acid (Figures 4A and S7). Collectively, these findings imply that AecE mediates linkage of **14** to AecC to form **17**. The acyl group of **17** is then transferred to the PKS AecD to initiate carbon chain elongation whereupon five rounds of chain extension lead to the production of **24** (Figure 3C). It is also noted that AecD lacks a thioesterase (TE) domain. Thus, the offloading of **24** from the ACP domain may be catalyzed by AecG, which is annotated as an α/β hydrolase and thus may serve as

a *trans*-acting thioesterase. However, this activity could not be verified since AecG forms inclusion bodies upon overexpression.

PKS-mediated formation of **24** renders subsequent oxidation at C11 unnecessary leaving epoxide installation as the remaining step in aerocyanidin biosynthesis. As mentioned above, the only uncharacterized oxidase gene in the *aec* cluster is *aecF*, which has been annotated as a cupin-domain-containing protein. This class of proteins is known to bind transition metals in their conserved β-barrel structures[16] and catalyze oxygenation reactions.[17,18] In addition, a BLAST search suggests that the cupin domain of AecF resembles the JmjC domain that is found in Fe/α-KG enzymes.[19] HHpred analysis[20] consistently revealed the Fe/α-KG halogenase OocP (PDB ID: 8A82) as a top hit for AecF. Therefore, AecF was hypothesized to be responsible for catalyzing the epoxidation of **24** to form **1.** However, recombinant AecF could not be expressed in *E. coli* as a soluble protein. Therefore, in vivo experiments were performed in which *aecF* was deleted inframe from the producing strain *C. violaceum*. Upon deletion of *aecF*, the production of **1** was abolished in the mutant strain (Figure 4B), whereas complementation of *aecF* into the Δ*aecF* mutant strain restored aerocyanidin production albeit not to the extent of the wild type (Figure 4B). This partial restoration could be due to a decrease in the expression level of the *aecF* gene in the complementation strain or another effect related to the *trans*-expression system. In addition, compound **24** was also observed to accumulate in the culture broth of the Δ*aecF* mutant strain as well as the *aecF* complementation strain but at a reduced level (ca. 20% that from the Δ*aecF* mutant strain); however, **24** was not observed with the wildtype strain (Figure 4C). This is consistent with the reduced production level of **1** in the *aecF* complementation strain as opposed to the wild type and the conclusion that AecF catalyzes the epoxidation of **24** to yield the final product **1.** However, the possibility that AecF acts prior to offloading of the carbon chain of **24** from AecD cannot yet be excluded.

The fact that aerocyanidin (**1**) and amycomicin (**3**) share similar structures and partially conserved gene clusters implies that biosynthesis of the core structure of **3** may be similar to that of **1.** As proposed in Figure 5, 2-hexenoyl-ACP (fatty acyl carrier protein or its CoA derivative) (**25**) could be sequentially processed by the bifunctional thioesterase AmcD and the Fe/α-KG enzyme AmcA to form the isonitrile intermediate **29** (**25** → **27** → **29**, Figure 5). The ligase AmcH may then catalyze loading of **29** onto the ACP AmcE (**29** → **31**, Figure 5). The PKSs AmcF and AmcG would accept and process **31** to afford the 18-carbon chain product **37** (**31** → **33** → **35** → **37**, Figure 5). While a homologue of *aecF* is absent in the *amc* cluster, the cluster instead encodes three putative P450 enzymes (i.e., *amcB*, *amcC*, and *amcQ*), which may be responsible for oxidative installation of the epoxide, the C8 keto and the C16 alkene functionalities (**37** → **3**, Figure 5).

Consistent with this proposal, the glycine adduct **27** was found to be generated when the SNAc analog (**39**) of 2-hexenoyl-ACP was synthesized and incubated with glycine and AmcD (Figure S8A). Moreover, **27** was converted in the presence of AmcA to the isonitrile product **29** (Figure S8A), which could be loaded onto AmcE in the presence of AmcH to give **31** (Figure S8B). However, one-pot reaction of chemically synthesized **29** with AmcE, AmcH, and the two PKS gene products AmcF and AmcG did not give rise to the expected

chain-elongated product **37** (Figure 6B). Instead, **44** (calcd for $C_{17}H_{30}NO_3^-$ [M−H]$^-$: 296.2231, found: 296.2232) was found to be the major product, the carbon chain of which is two carbons shorter than **37** and **3** (see Figures 6B and S9 for the structure of **44**). This observation indicated that the final round of elongation to extend a 16-carbon chain to an 18-carbon chain (**44** → **37**) did not happen, probably due to the inability of the ketosynthase (KS) domain of AmcF or AmcG to accommodate the 16-carbon chain substrate for another round of elongation (Figure S9A). Accordingly, **31** may not be the true starter unit for PKS elongation, and 2-hexenoyl-ACP (**25**) is not the precursor for amycomicin biosynthesis. These observations prompted us to consider an alternative starter unit of chain elongation catalyzed by AmcF.

As mentioned earlier, the *amc* cluster also contains an additional set of genes that are related to FAB (see Figure 2A). These include the ACP *amcJ*, the two *fabF* (ketosynthase for chain elongation) homologues *amcK* and *amcL*, the *fabA* (dehydratase) homologue *amcM*, the *fabZ* (dehydratase) homologue *amcN*, the *fabG* (ketoreductase) homologue *amcO*, and the *fabH* (ketosynthase for initiation of FAB) homologue *amcS*. Therefore, the enzymes encoded by these genes may play an important role in the construction of the productive six-carbon starter unit used in the chain initiation of amycomicin biosynthesis. Based on their annotations, these FAB enzymes may produce 2,4-hexadienoyl-ACP, also known as sorbic-ACP (**26**) (Figure 6A), which could potentially serve as the six-carbon precursor for the biosynthesis of amycomicin (Figure 5).

To investigate this biosynthetic model, the SNAc analog (**45**) of sorbic-ACP (**26**), was synthesized and tested. As shown in Figure S10, **45** can be processed by AmcD, AmcA, and AmcE/AmcH in sequence to form **30** and then **32.** More importantly, incubation of a synthetic racemate of **30** with AmcE, AmcH, AmcF and AmcG successfully produced the chain-elongated product **38** (calcd for $C_{19}H_{32}NO_3^-$ [M−H]$^-$: 322.2388, found: 322.2396) with the correct chain length of 18 carbons (Figures 6C and S11D). This result showed **32** to be the starter unit for PKS elongation catalyzed by AmcF, thereby indicating that sorbic-ACP (**26**) is the true entry point to amycomicin biosynthesis. Omitting AmcG from the above reaction led to no production of **38** but accumulation of **46** (calcd for $C_9H_{12}NO_3^-$ [M−H]$^-$: 182.0823, found: 182.0835) and **47** (calcd for $C_{11}H_{16}NO_3^-$ [M−H]$^-$: 210.1136, found: 210.1150) (Figures 6C and S11B,C). These findings suggested that the ten-carbon acyl chain of **47** cannot be accepted by the KS domain of AmcF but requires the standalone KS AmcG to catalyze further elongation (Figure S11A).

Having established the assembly of the 18-carbon chain intermediate **38**, the subsequent installations of the epoxide and the keto group are believed to be catalyzed by the three P450 enzymes, AmcB, AmcC and AmcQ. To interrogate the roles of these P450 enzymes, a synthetic racemate of **38** was incubated with AmcB, AmcC or AmcQ individually along with other necessary reaction components (see Supporting Information). LCMS analysis of the reaction mixture of AmcQ with **38** showed that **38** was depleted with concomitant formation of four oxygenated species, **P1, P2, P3** and **P4** (Figure 7B). According to the *m*/*z* values, **P1** (calcd for $C_{19}H_{32}NO_4^-$ [M−H]$^-$: 338.2337, found: 338.2345) can be assigned as the monohydroxylated product (+16 Da) of **38**, while **P2** (calcd for $C_{19}H_{30}NO_4^-$ [M−H]$^-$:

336.2180, found: 336.2185) is the dehydrogenated product (−2 Da) of **P1**. Furthermore, **P3** (calcd for $C_{19}H_{30}NO_5^-$ $[M-H]^-$: 352.2129, found: 352.2120) may result from hydroxylation of **P2**, and **P4** (calcd for $C_{19}H_{28}NO_5^-$ $[M-H]^-$: 350.1973, found: 350.1967) is the dehydrogenated product of **P3.** Time course analysis of the AmcQ assay revealed that **38** undergoes two consecutive rounds of hydroxylation and dehydrogenation to form **P4** (**38** → **P1** → **P2** → **P3** → **P4**, Figure S12). However, attempts to isolate and characterize these products were unsuccessful perhaps due to their instability and scarcity.

Three isotopologs of **38** including [8-^{2}H]-**38**, [14-$^2H_2$]-**38**, and [15-^{2}H]-**38**, all in their racemic forms, were synthesized in order to probe the loci where oxidation takes place in AmcQ catalyzed reactions. Retention of deuterium labels were observed in all four products (**P1** to **P4**) when [14-$^2H_2$]-38 or [15-^{2}H]-38 was used as the substrate (Figure S13C,D) indicating that C14 and C15 are not affected by the AmcQ catalyzed reaction. In contrast, reaction of AmcQ with [8-^{2}H]-**38** led to partial retention of 8-^{2}H in P1 and disappearance from **P2**, **P3** and **P4** (Figures 7C and S13B). These results suggested that AmcQ first catalyzes hydroxylation at C8 to form **P1** followed by dehydrogenation to generate the C8 keto product **P2**. While the site of subsequent hydroxylation and dehydrogenation to yield **P3** and **P4** was not determined, it must be at a carbon other than C14 or C15. To uncover the source of the oxygen atoms, ^{18}O-isotope tracer experiments with $^{18}O_2$ and $H_2{}^{18}O$ were performed. The results shown from Figure S14A to C demonstrated that molecular oxygen is incorporated once into **P1** and **P2** as well as twice into **P3** consistent with the mechanism of P450-catalyzed oxygenation.[21] In contrast, H_2O was incorporated at both sites in **P4** (Figure S14D). As **P4** is the dehydrogenated product of **P3**, it is likely that **P4** bears two keto groups including the one at C8, which are prone to solvent exchange.

Despite the fact that AmcQ catalyzes C8 hydroxylation and dehydrogenation of **38** to yield the ketone **P2**, the overoxidation of **P2** to **P3** and **P4** suggested that **38** may not be the true substrate for AmcQ. Instead, epoxidation of **38** between C14 and C15 may occur prior to C8 oxygenation. The remaining two P450 enzymes AmcB and AmcC are thus hypothesized to catalyze the epoxidation step. To test this hypothesis, AmcB-AmcC coupled reaction with **38** was conducted. However, the anticipated epoxidation product (**51**) was not detected by LCMS analysis. Rather, a new peak was observed eluting at 10.8 min (**P5**) (traces i and iv, Figure 8B). By comparison with the authentic standard, **P5** was established to be 13-hydroxytridecanoic acid (**52**, traces iv and v, Figure 8B). When [8-^{2}H]-**38** was used as the substrate, the mass of **P5** increased by 1 Da (Figure S15), suggesting that **P5** is indeed derived from **38.** It is noteworthy that incubation of **38** with either AmcB or AmcC alone also generated **P5** but with much lower efficiency (traces ii to iv, Figure 8B). Collectively, these results suggest that **38** is transformed to an unstable product in the presence of AmcB and AmcC, which rapidly decomposes to **P5** (**52**) presumably via C−C bond breakage between C13 and C14. The details regarding this process are still under investigation.

Given the transient nature of the AmcB-AmcC product, one-pot reaction of **38** with AmcB, AmcC, and AmcQ was carried out. However, the major products from this one-pot assay were **P3** and **P4** without any previously unnoticed products (Figure S16), indicating that a majority of the substrate had been consumed by AmcQ without the involvement of AmcB

or AmcC. To overcome this, **38** was first incubated with AmcB and AmcC for 10 min before adding AmcQ. After another 20 min, enzymes were removed by centrifugal filtration. LCMS analysis of the reaction filtrate revealed a new EIC peak (**P6**, calcd for $C_{19}H_{28}NO_5^-$ $[M-H]^-$: 350.1973, found: 350.1967) (Figure 8C), the molecular weight of which is 28 Da greater than **38** consistent with the addition of two oxygen atoms, loss of four hydrogen atoms and thus the structure of amycomicin (3). While significant amounts of **P1, P2**, and **P3** were also generated, **P5** was not detected (Figure S17). This suggests that the product of the AmcB-AmcC reaction was not degraded to **P5** but very likely converted to **P6** by AmcQ. Consistent with this hypothesis, incubation of **38** with AmcQ followed by ultrafiltration to remove AmcQ prior to addition of AmcB and AmcC did not generate **P6** (Figure S18), indicating that **38** must first be processed by AmcB and AmcC before AmcQ to produce **P6.**

To determine the source of the two added oxygen atoms, the reaction was run with $^{18}O_2$ (97 atom %)/$H_2{}^{16}O$ and $^{16}O_2/H_2{}^{18}O$ (65 atom %). Incorporation of two ^{18}O isotopes into **P6** from $^{18}O_2$ were observed while no ^{18}O incorporated from $H_2{}^{18}O$ was detected (Figure S14E). Moreover, these two oxygens are proposed to include one at C8 as a keto group and the other between C14 and C15 as an epoxide. Due to its extreme instability, preparation of an amycomicin standard for direct comparison with **P6** proved challenging. Thus, site-specifically deuterated **38**, including [8-^{2}H]-**38**, [14-$^2H_2$]-**38**, and [15-^{2}H]-**38** were respectively assayed to establish the position of hydrogen abstraction from **38** to form **P6.** As a result, the deuterium in [8-^{2}H]-**38** was completely lost in **P6** (spectrum ii, Figure 8D) consistent with formation of a ketone at C8. Furthermore, only one deuterium was lost from the [14-$^2H_2$]-**38** while the deuterium in [15-^{2}H]-**38** was found to be completely depleted (spectra iii and iv, Figure 8D). This is consistent with addition of the second oxygen as an epoxide bridging C14 and C15 and thus the assignment of **P6** as **3**. Therefore, the final steps in amycomicin biosynthesis are established to involve the AmcB-AmcC catalyzed epoxidation of **38** between C14 and C15 followed by AmcQ catalyzed hydroxylation and dehydrogenation of C8 (**38** → **51** → **3**, Figure 8A).

Several putative mechanisms regarding the epoxidation catalyzed by the P450 enzymes AmcB/C can be envisioned as shown in Figures 9 and S19. The reactive Compound (Cpd) I may abstract the hydrogen atom at C14 followed by hydroxyl rebound to give **54** (**38** → **53** → **54**, Figure 9). The second hydrogen atom abstraction could be performed at C15 in **54** by a second Cpd I to result in the C15 radical **55.** Oxidation of the C15 radical by Cpd II followed by cyclization could form the epoxide **51** (**55** → **51**, Figure 9). Alternatively, the initial C14 radical **53** could undergo one-electron oxidation then deprotonation of C15 to yield a double bond between C14 and C15 (**53** → **56**, Figure 9). Oxygen atom transfer from the second Cpd I to the C14=C15 double bond would generate **51** (**56** → **51**, Figure 9). Analogous reaction pathways beginning with hydrogen atom abstraction from C15 of **38** are also possible (see Figure S19).

CONCLUSIONS

In summary, the biosynthetic pathways of aerocyanidin (**1**) and amycomicin (**3**) have been fully elucidated in this work. Both share the conserved INLP mechanism of isonitrile functionalization in **14** and **30.** Unlike the NRPS machinery at work in the production of

INLPs, the acyl group of the AecC-bound isonitrile intermediate **17** is transferred to the PKS enzyme AecD (**17** → **18**, Figure 3C) to undergo carbon chain extension in the assembly of aerocyanidin (**1**). The first round of elongation generates the β-hydroxy product **19**, which accounts for the formation of the C11 hydroxyl group in **1.** The following four rounds of fully reducing elongation and hydrolysis yield **24.** Finally, the cupin domain-containing protein AecF catalyzes epoxidation to conclude the biosynthesis of **1.** Construction of the isonitrile PKS starter unit during the biosynthesis of amycomicin is initiated with sorbic-ACP (**26**) which is a product of fatty acid biosynthesis. The following steps encompass reactions sequentially catalyzed by AmcD, AmcA, and AmcE/AmcH such that the starting material **26** is transformed to **32.** Distinct from that in aerocyanidin biosynthesis where a single PKS is sufficient for the chain extension, the standalone KS AmcG is required in addition to the PKS AmcF to accomplish the conversion from **32** to **38**. Specifically, AmcG is indispensable for the third round of elongation. Furthermore, unlike aerocyanidin biosynthesis, the cytochrome P450 enzymes AmcB and AmcC catalyze epoxidation of **38** to **51.** Finally, the third P450 enzyme, AmcQ, catalyzes the keto formation at C8 to conclude the biosynthesis of **3** (**51** → **3**).

Fatty acid chains serve as the template for isonitrile formation during the biosynthesis of INLPs such as INLP-2 (**8**). This is followed by introduction of the peptide linkages to complete the production of these isonitrile-containing lipopeptides. Likewise, construction of the isonitrile moiety during the biosynthesis of aerocyanidin (**1**) and amycomicin (**3**) also occurs on a fatty acyl precursor. However, the subsequent chain elongation to assemble the hydrocarbon chain in the final structures are catalyzed by polyketide synthases in both cases. Importantly, these studies reveal that formation of the γ-hydroxy group in **1** and **3** are generated during PKS catalyzed chain elongation, and the olefinic moiety in **3** is from construction of the fatty acyl starter unit by FAB enzymes. All of them are not tailoring oxidation reactions as previously proposed. These findings thus help explain the apparent deficiency of oxidase genes in the *aec* and *amc* gene clusters. This work also demonstrates that biosynthesis of the epoxide group in **1** and **3** involves two different pathways. While accessing the epoxy isonitrile functionality synthetically has been challenging,[22] this study unravels two distinctive enzymatic routes to introduce an epoxide at the aliphatic position α,β to an isonitrile group. These findings may be of use in developing a biocatalytic approach to the epoxy isonitrile moiety, which is a potentially useful pharmacophore.

Supplementary Material

Refer to Web version on PubMed Central for supplementary material.

ACKNOWLEDGMENTS

The heterologous expression host *E. coli* K207 was generously provided by Prof. Adrian Keatinge-Clay at the University of Texas at Austin. The plasmids *camA*/pET28b(+) and *camB*/pET28b(+) for expressing CamA and CamB proteins for P450 enzyme assays were kindly provided by Prof. Ikuro Abe at the University of Tokyo. We are grateful to Dr. Kazuo Shin-ya at the National Institute of Advanced Industrial Science and Technology for searching for the producing strain of YM-47515. We thank Dr. Daan Ren for providing the Sfp protein, and Dr. Yu-Hsuan Lee and Joseph Livy Franklin for providing the MatB protein. We thank Dr. Mark Ruszczycky for his valuable comments on this manuscript. This work was supported by the National Institutes of Health (GM040541 to H.-w.L. and R01AT009874 to J.C.).

REFERENCES

(1). Parker WL; Rathnum ML; Johnson JH; Wells JS; Principe PA; Sykes RB Aerocyanidin, a new antibiotic produced by *Chromobacterium violaceum*. J. Antibiot 1988, 41 (4), 454–460.

(2). Sugawara T; Tanaka A; Imai H; Nagai K; Suzuki K YM-47515, a novel isonitrile antibiotic from *Micromonospora echinospora* subsp. *echinospora*. J. Antibiot 1997, 50 (11), 944–948.

(3). Pishchany G; Mevers E; Ndousse-Fetter S; Horvath DJ; Paludo CR; Silva EA; Koren S; Skaar EP; Clardy J; Kolter R Amycomicin is a potent and specific antibiotic discovered with a targeted interaction screen. Proc. Natl. Acad. Sci. U. S. A 2018, 115 (40), 10124–10129. [PubMed: 30228116]

(4). Ernouf G; Wilt IK; Zahim S; Wuest WM Epoxy isonitriles, a unique class of antibiotics: synthesis of their metabolites and biological investigations. ChemBioChem. 2018, 19 (23), 2448–2452. [PubMed: 30277650]

(5). Tamura A; Kotani H; Naruto S Trichoviridin and dermadin from *Trichoderma* sp. TK-1. J. Antibiot 1975, 28 (2), 161–162.

(6). Ollis WD; Rey M; Godtfredsen WO; Rastrupandersen N; Vangedal S; King TJ The constitution of the antibiotic trichoviridin. Tetrahedron 1980, 36 (4), 515–520.

(7). Sood M; Kapoor D; Kumar V; Sheteiwy MS; Ramakrishnan M; Landi M; Araniti F; Sharma A Trichoderma: the ″secrets″ of a multitalented biocontrol agent. Plants 2020, 9 (6), 762. [PubMed: 32570799]

(8). Baldwin JE; Adlington RM; Oneil IA; Russell AT; Smith ML The total synthesis of (±)-trichoviridin. Chem. Commun 1996, 41–42.

(9). Harris NC; Sato M; Herman NA; Twigg F; Cai W; Liu J; Zhu X; Downey J; Khalaf R; Martin J; Koshino H; Zhang W Biosynthesis of isonitrile lipopeptides by conserved nonribosomal peptide synthetase gene clusters in Actinobacteria. Proc. Natl. Acad. Sci. U.S.A 2017, 114 (27), 7025–7030. [PubMed: 28634299]

(10). Harris NC; Born DA; Cai W; Huang Y; Martin J; Khalaf R; Drennan CL; Zhang W Isonitrile formation by a nonheme iron(II)-dependent oxidase/decarboxylase. Angew. Chem., Int. Ed 2018, 57 (31), 9707–9710.

(11). Chen T-Y; Zheng Z; Zhang X; Chen J; Cha L; Tang Y; Guo Y; Zhou J; Wang B; Liu H.-w.; Chang W-C. Deciphering the reaction pathway of mononuclear iron enzyme-catalyzed N≡C triple bond formation in isocyanide lipopeptide and polyketide biosynthesis. ACS Catal. 2022, 12 (4), 2270–2279. [PubMed: 35992736]

(12). Wilson MC; Moore BS Beyond ethylmalonyl-CoA: the functional role of crotonyl-CoA carboxylase/reductase homologs in expanding polyketide diversity. Nat. Prod. Rep 2012, 29 (1), 72–86. [PubMed: 22124767]

(13). Bhushan R; Bruckner H Marfey's reagent for chiral amino acid analysis: a review. Amino Acids 2004, 27 (3−4), 231–247. [PubMed: 15503232]

(14). Keatinge-Clay AT; Stroud RM The structure of a ketoreductase determines the organization of the β-carbon processing enzymes of modular polyketide synthases. Structure 2006, 14 (4), 737–748. [PubMed: 16564177]

(15). Khosla C; Tang Y; Chen AY; Schnarr NA; Cane DE Structure and mechanism of the 6-deoxyerythronolide B synthase. Annu. Rev. Biochem 2007, 76, 195–221. [PubMed: 17328673]

(16). Dunwell JM; Culham A; Carter CE; Sosa-Aguirre CR; Goodenough PW Evolution of functional diversity in the cupin superfamily. Trends Biochem. Sci 2001, 26 (12), 740–746. [PubMed: 11738598]

(17). Ng TL; Rohac R; Mitchell AJ; Boal AK; Balskus EP An *N*-nitrosating metalloenzyme constructs the pharmacophore of streptozotocin. Nature 2019, 566 (7742), 94–99. [PubMed: 30728519]

(18). He H-Y; Henderson AC; Du Y-L; Ryan KS Twoenzyme pathway links L-arginine to nitric oxide in *N*-nitroso biosynthesis. J. Am. Chem. Soc 2019, 141 (9), 4026–4033. [PubMed: 30763082]

(19). Klose RJ; Kallin EM; Zhang Y JmjC-domain-containing proteins and histone demethylation. Nat. Rev. Genet 2006, 7 (9), 715–727. [PubMed: 16983801]

(20). Alva V; Nam SZ; Söding J; Lupas AN The MPI bioinformatics toolkit as an integrative platform for advanced protein sequence and structure analysis. Nucleic Acids Res. 2016, 44 (W1), W410–W415. [PubMed: 27131380]

(21). Meunier B; de Visser SP; Shaik S Mechanism of oxidation reactions catalyzed by cytochrome P450 enzymes. Chem. Rev 2004, 104 (9), 3947–3980. [PubMed: 15352783]

(22). Baldwin JE; Chen DQ; Russell AT On the synthesis of vinyl isonitriles. Chem. Commun 1997, 2389–2390.

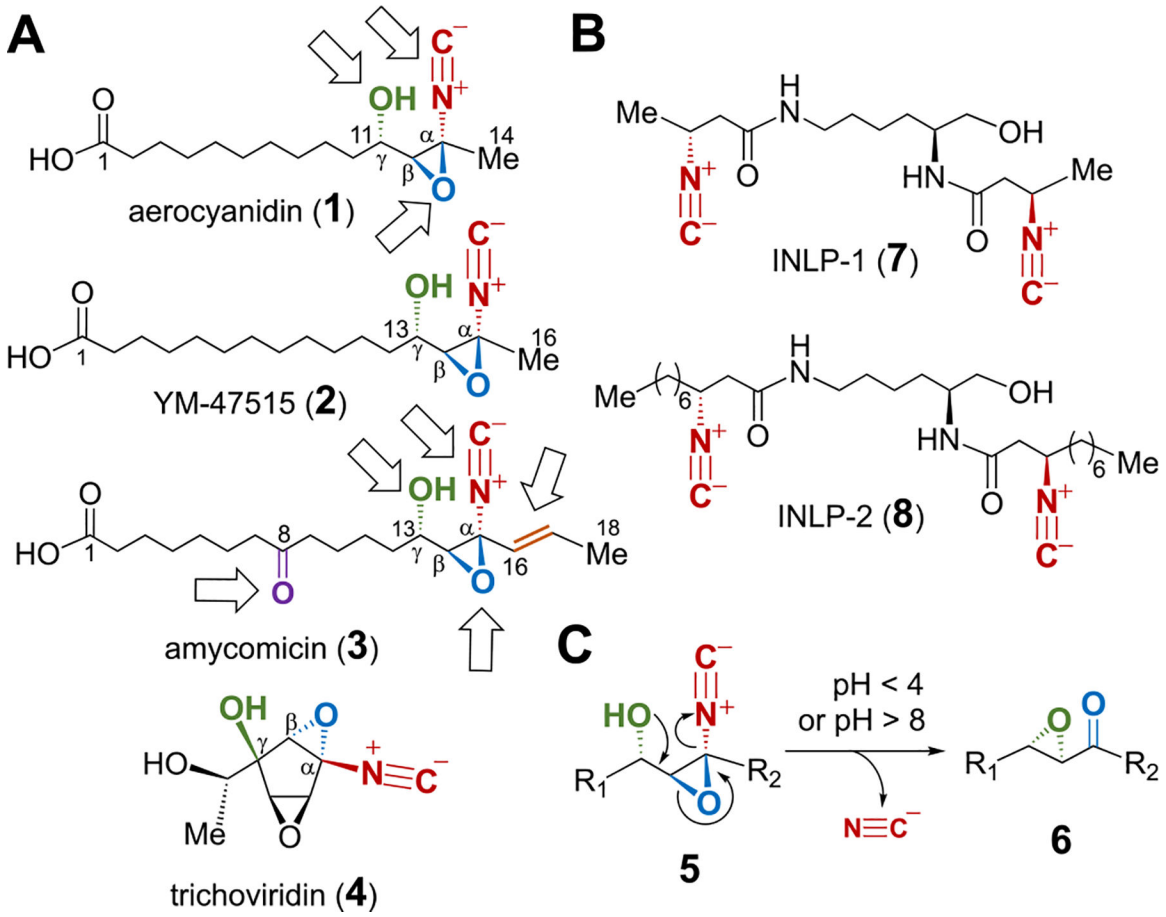

Figure 1.

(A) Epoxy isonitrile-containing antibiotics. Arrows indicate the oxidative modifications on the long-chain acid backbone in **1** and **3**. (B) Isonitrile-containing lipopeptides. (C) Payne rearrangement as a part of decomposition of the epoxy isonitrile functionality.

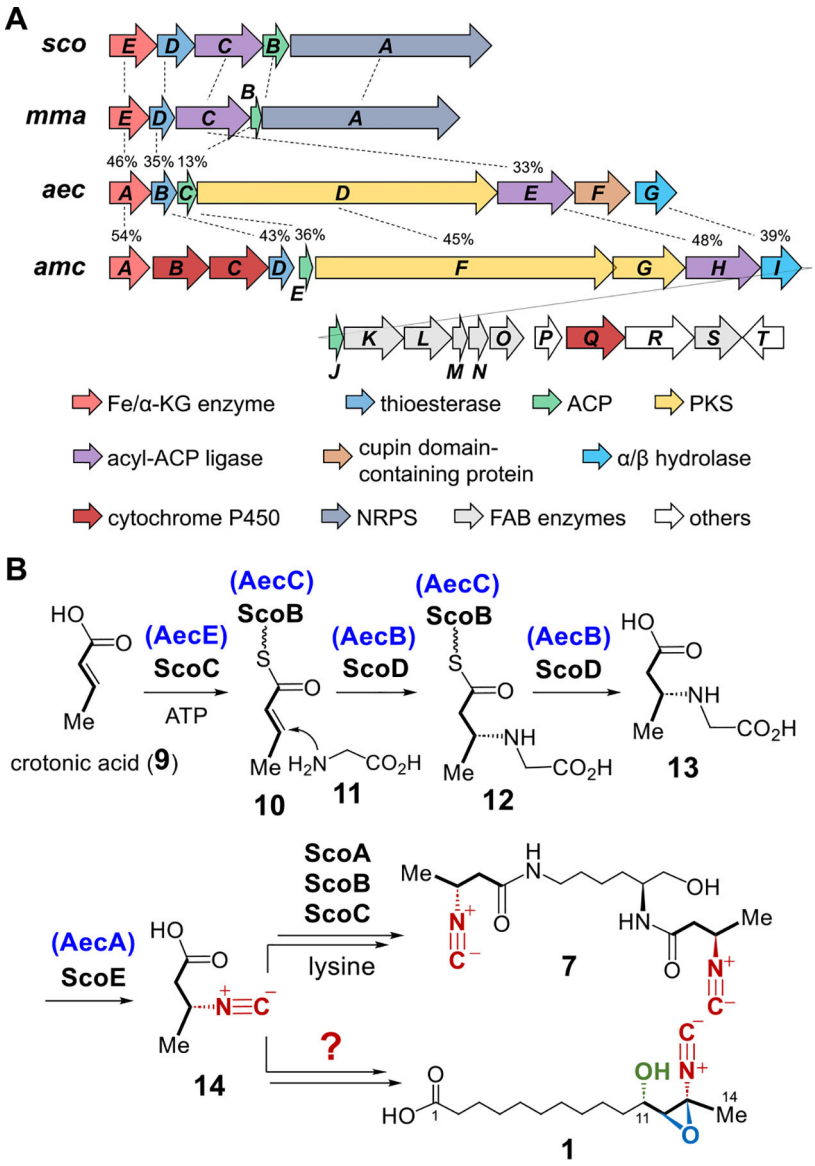

Figure 2.

(A) Gene clusters for INLP-1 (**7**) (*sco*), INLP-2 (**8**) (*mma*), aerocyanidin (**1**) (*aec*), and amycomicin (**3**) (*amc*). Percentages indicate the sequence identity between the two homologous genes. (B) Biosynthesis of **7** and **1** may share the same intermediate **14**.

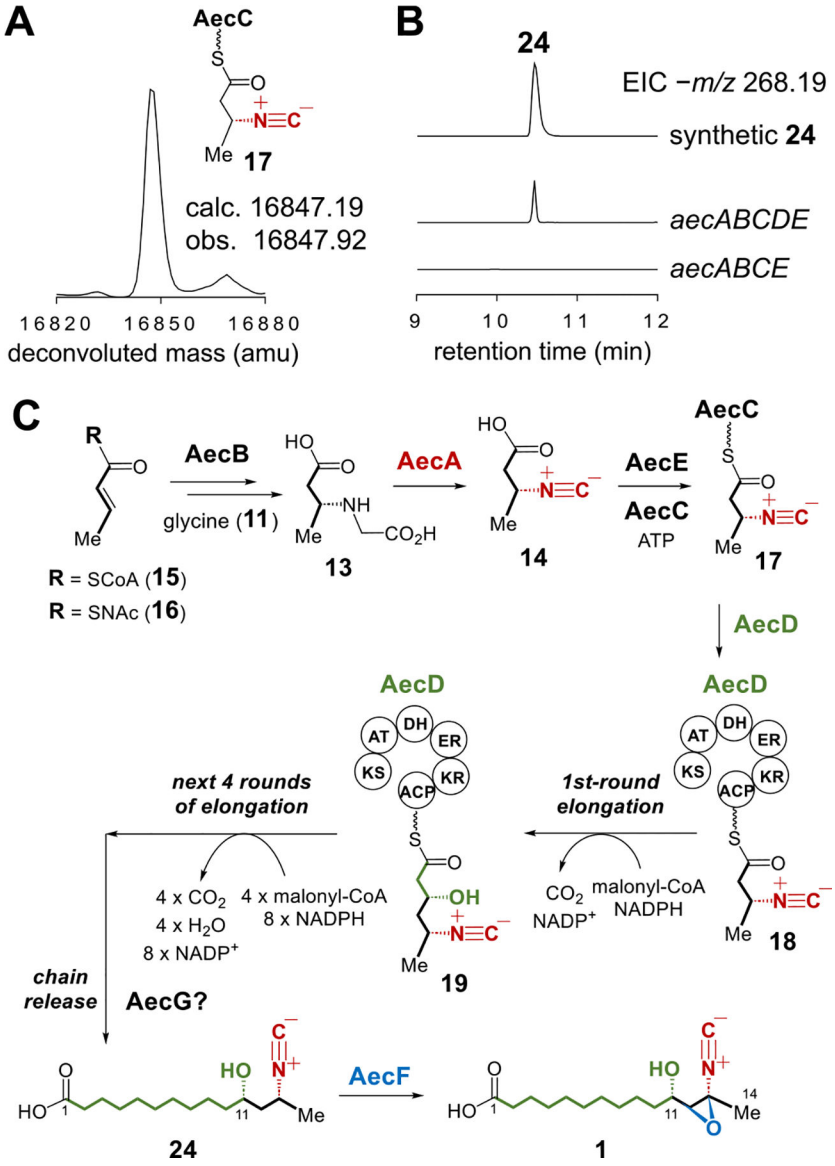

Figure 3.

(A) MS analysis of **17**. (B) LCMS analysis of the heterologous expression experiments of *aecABCDE*. (C) Proposed biosynthetic pathway of aerocyanidin (**1**).

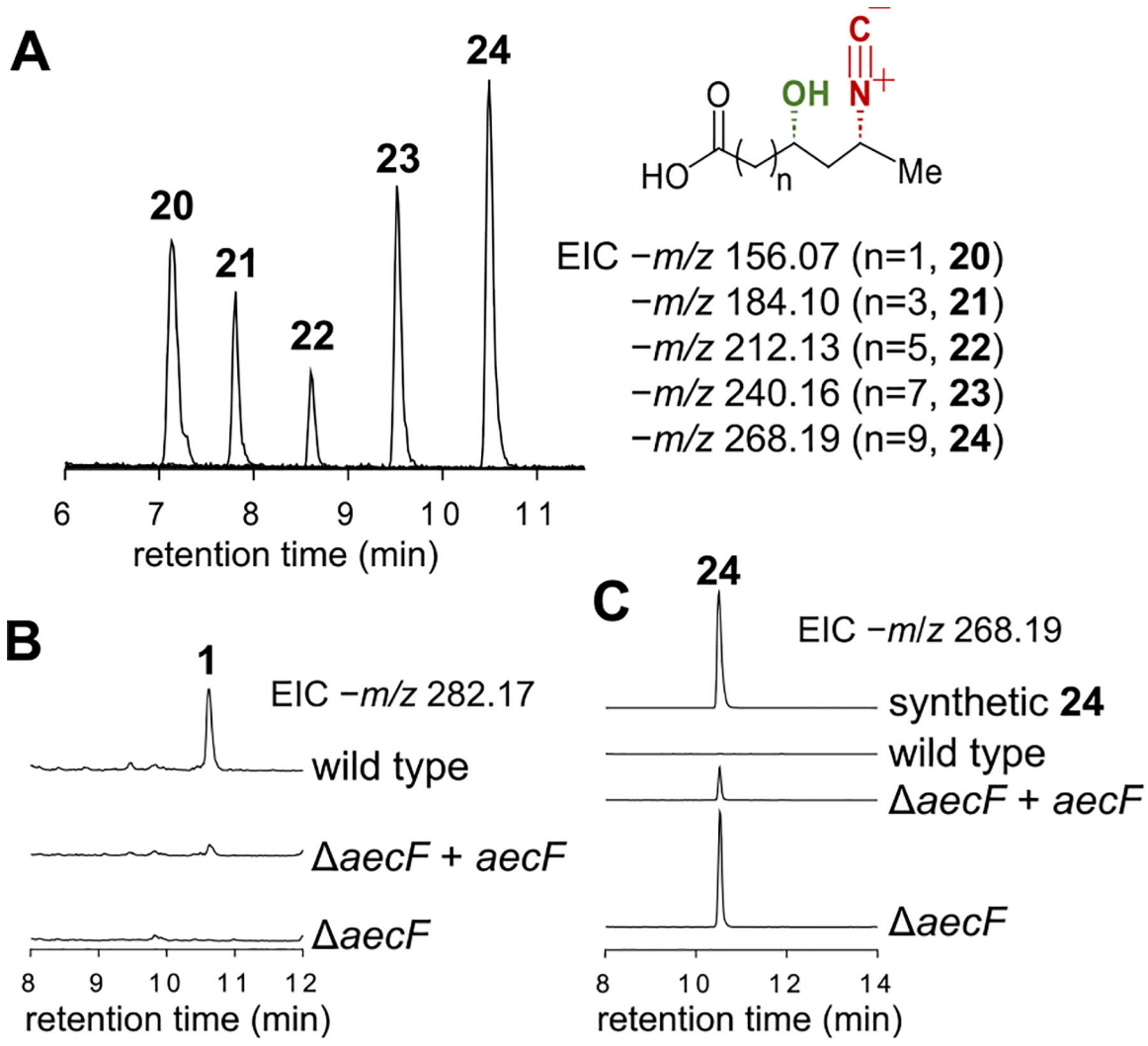

Figure 4.

(A) LCMS analysis of the in vitro AecD reaction. (B, C) LCMS analysis of the gene deletion and complementation experiments of *aecF*.

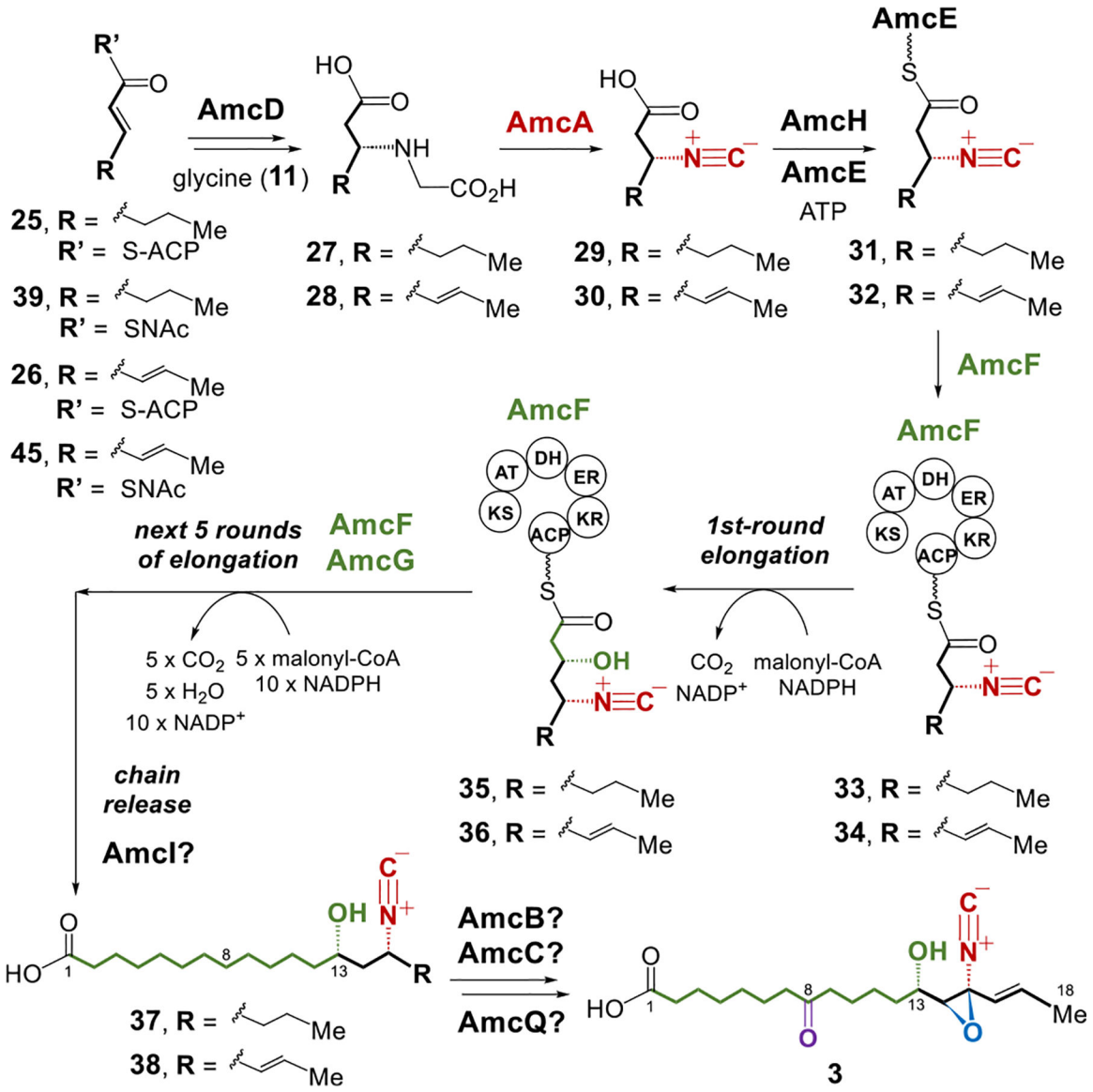

Figure 5.
Proposed biosynthetic pathways of amycomicin (**3**).

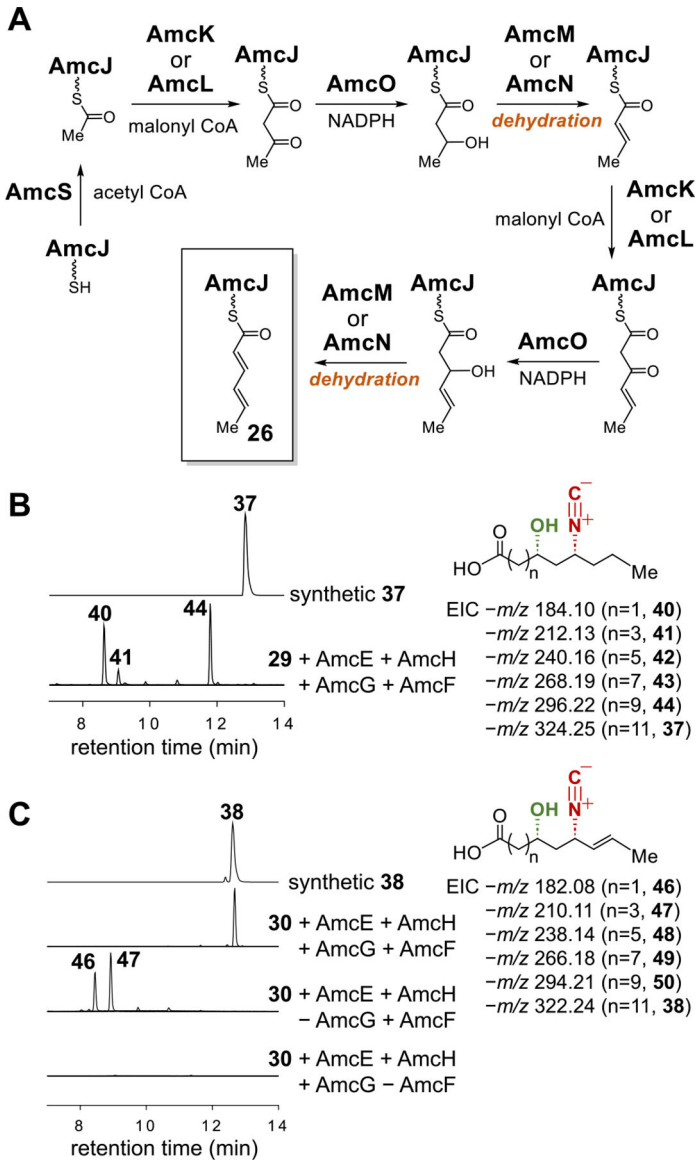

Figure 6.

(A) Proposed biosynthetic pathway for sorbic-ACP (**26** with AmcJ serving as ACP). (B) LCMS analysis of the in vitro PKS reaction with **29** and (C) with **30**.

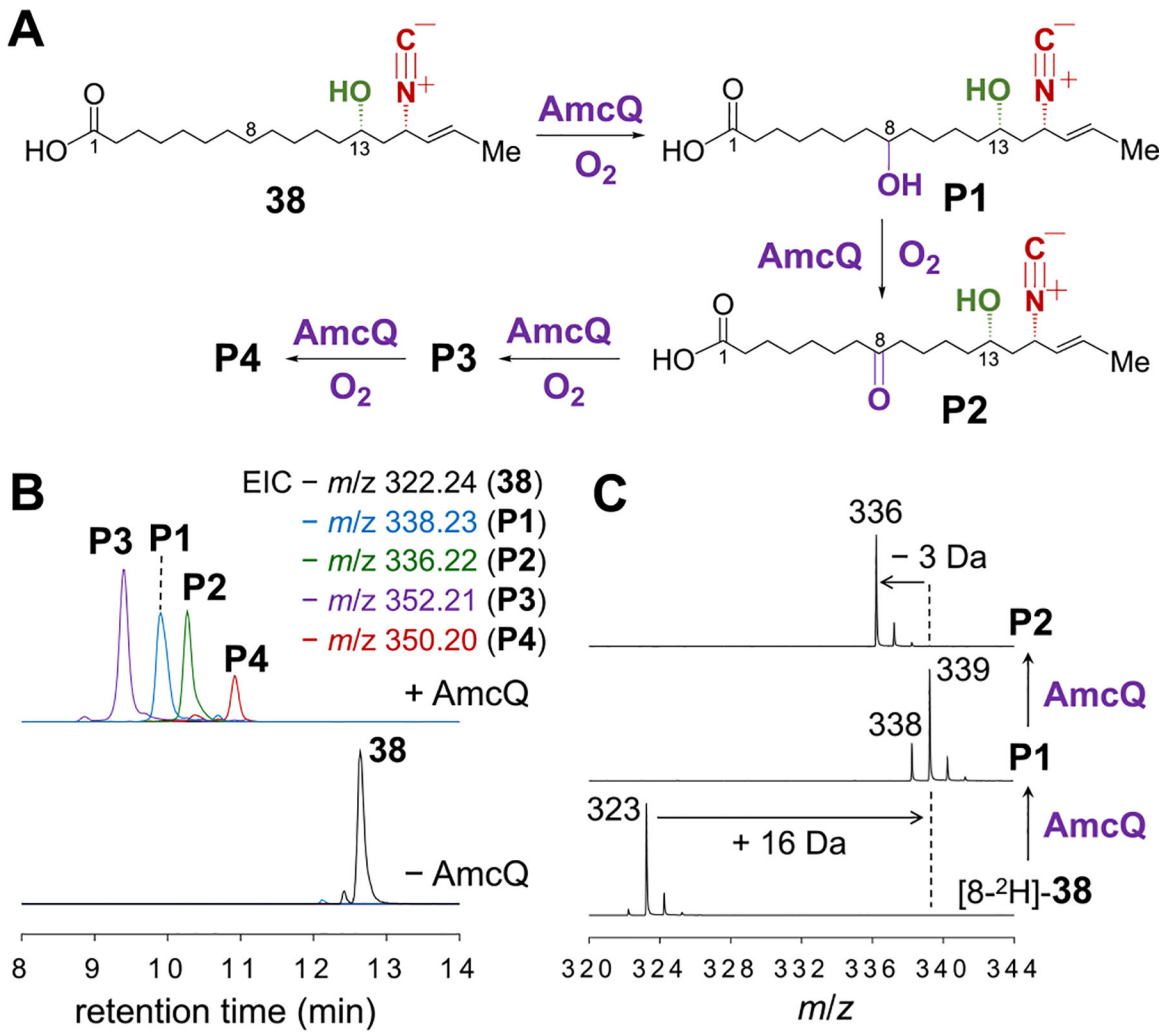

Figure 7.

(A) Scheme and (B) LCMS analysis of the AmcQ reaction with **38.** (C) Mass analysis of **P1** and **P2** generated in the AmcQ reaction with [8-^{2}H]-**38.**

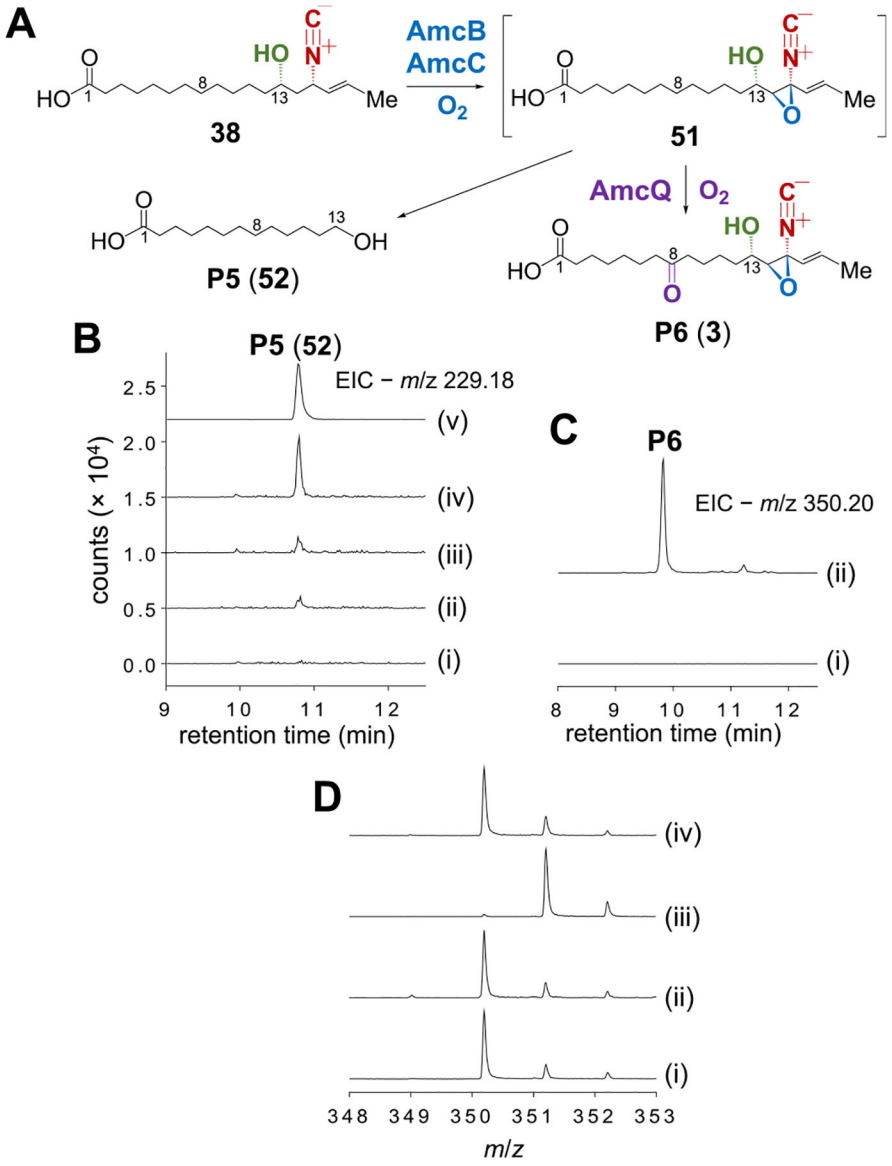

Figure 8.

(A) Scheme of the final steps in amycomicin (**3**) biosynthesis involving AmcB, AmcC and AmcQ. (B) LCMS analysis of the AmcB-AmcC reaction with **38:** (i) without AmcB or AmcC; (ii) with AmcB only; (iii) with AmcC only; (iv) with both AmcB and AmcC; (v) standard of **52.** (C) LCMS analysis of the AmcB-AmcC-AmcQ coupled reaction with **38:** (i) incubation of **38** with AmcB and AmcC for 30 min; (ii) incubation of **38** with AmcB and AmcC for 10 min followed by addition of AmcQ and incubation for another 20 min. (D) Mass analysis of **P6** produced in the AmcB-AmcC-AmcQ coupled reaction with (i) unlabeled **38**, (ii) [8-^{2}H]-**38**, (iii) [14-$^{2}H_2$]-**38**, and (iv) [15-^{2}H]-**38**.

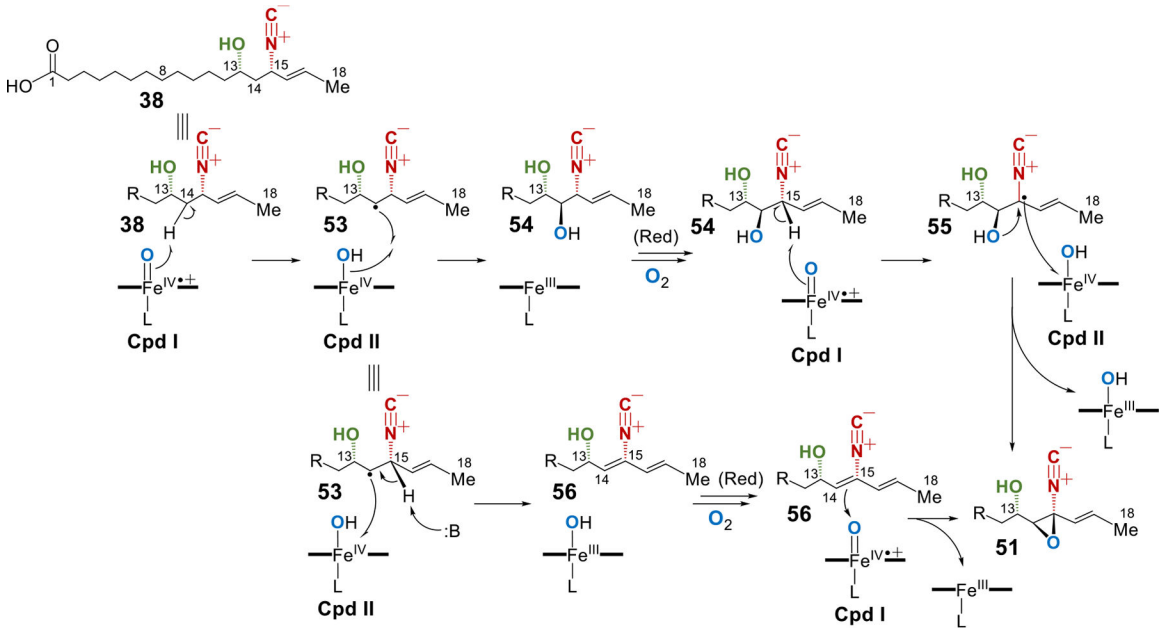

Figure 9.

Proposed mechanisms for the AmcB/C catalyzed epoxidation involving the first hydrogen atom abstraction at C14 of **38.** [Red] stands for the reduction that is required for the resting Fe(III) complex to react with O_2 to form Cpd I.